Evaluation of Tribological and Electrochemical Properties of Multiphase CoCuFeNiNb High Entropy Alloy

Sefa Emre Sünbül[1] [iD], Kürşat İçin[2] [iD]

[1]Gaziantep Üniversitesi, Mühendislik Fakültesi, Metalurji ve Malzeme Mühendisliği, Gaziantep
[2]Karadeniz Teknik Üniversitesi, Mühendislik Fakültesi, Metalurji ve Malzeme Mühendisliği, Trabzon

Abstract

Recent research has heavily focused on high entropy alloys (HEAs) due to their promising potential for diverse industrial applications. This study investigates the CoCuFeNiNb alloy, analyzing its structural, tribological, and electrochemical characteristics. The alloy was synthesized using vacuum arc melting in an argon environment and was subsequently examined through X-ray diffraction (XRD), scanning electron microscopy (SEM), energy dispersive X-ray spectroscopy (EDX), wear testing, and corrosion analysis. The tribological and electrochemical performances were assessed through wear and corrosion experiments. The results reveal that the alloy contains FCC, BCC, and Laves phases. The coefficient of friction for the CoCuFeNiNb high entropy alloy increased to 0.28, 0.5, and 0.78 under loads of 0.25 MPa, 0.5 MPa, and 1 MPa, respectively. Observations of the wear surface showed abrasion wear at low pressure, delamination layers at medium pressure, and plastic deformation zones at high pressure. In a 3.5 wt% NaCl solution, the alloy exhibited a corrosion potential of -0.236 V and a corrosion current density of 1.89×10^{-5} A/cm².

Keywords: high entropy alloy, vacuum arc melting, tribological properties, corrosion properties

Çok Fazlı CoCuFeNiNb Yüksek Entropili Alaşımın Tribolojik ve Elektrokimyasal Özelliklerinin Değerlendirilmesi

Öz

Yüksek entropili alaşımlar (YEA'lar), son yıllarda yoğun araştırmalara konu olmuş ve farklı endüstriyel uygulamalara yönelik potansiyel göstermektedir. Bu çalışma, CoCuFeNiNb alaşımının yapısal, tribolojik ve elektrokimyasal özelliklerini incelemektedir. Alaşım, Ar atmosferinde vakumlu ark eritme yöntemi ile hazırlanmış ve XRD, SEM, EDX, aşınma ve korozyon analizleri ile karakterize edilmiştir. Aşınma testleri ve korozyon deneyleri, alaşımın tribolojik ve elektrokimyasal performansını değerlendirmiştir. Bulgular, alaşımın YMK, HMK ve Laves fazlarından oluştuğunu göstermektedir. CoCuFeNiNb yüksek entropili alaşımının sürtünme katsayısı, 0.25 MPa, 0.5 MPa ve 1 MPa yük altında sırasıyla 0.28, 0.5 ve 0.78 olarak artış göstermiştir. Aşınma yüzeyinde düşük basınçta abrazyon izleri, orta basınçta delaminasyon tabakaları ve yüksek basınçta plastik deformasyon bölgeleri gözlemlenmiştir. CoCuFeNiNb alaşımının %3,5 NaCl çözeltisindeki korozyon potansiyeli -0,236 V ve korozyon akım yoğunluğu $1,89 \times 10^{-5}$ A/cm² olarak belirlenmiştir.

Anahtar Kelimeler: yüksek entropili alaşım, vakum ark ergime, tribolojik özellikler, korozyon özellikleri

Corresponding Author: Kürşat İçin ✉ kursaticin@ktu.edu.tr

Introduction

High entropy alloys (HEAs) have been intensively researched in literature for the last 20 years (Miracle & Senkov, 2017). Following the discovery of HEAs, they have gained great momentum in the scientific field and high entropy studies in various subjects are still popular. Like many other innovations, high entropy alloys need time to transition to industrial use or application. It is thought that all alloys and compounds in this series will find their place in the industry over time (Dada et al., 2023; Rashidy Ahmady et al., 2023).

The term HEA was first introduced in 2004 by Yeh and his research group (Chen et al., 2004; Yeh et al., 2004). Unlike conventional alloys, HEAs are formed with elements used in equal or close proportions (Sonar et al., 2024). Four main factors make high entropy alloys important: the high entropy effect (Dewangan et al., 2022), slow diffusion effect (Verma et al., 2024), lattice distortion (Wang et al., 2024), and cocktail effect (Wang et al., 2023). The high entropy effect reduces the free energy of solid solution phases in the alloy, facilitating their formation at high temperatures (Yu et al., 2024). The slow diffusion effect arises since each atom in each lattice site within the alloy is different from its neighboring atoms and this leads to different local energy levels within the lattice, hence diffusion is slow in HEAs (Verma et al., 2024). Lattice distortion occurs due to the atoms in the structure having different diameters (Wang et al., 2024). Finally, the cocktail effect refers to the dependence of the properties of the alloy on the properties of different elements (Cao et al., 2020). For example, Al, a light element, reduces the density of the alloy, while adding Al to CoCrCuFeNi alloy increases the hardness (Man et al., 2022; Yang et al., 2015; C. Zhang et al., 2023). Through the combination of five or more different elements, HEAs have the potential to produce a variety of properties

High entropy alloys are alloy groups with the potential to combine properties such as high strength and plasticity, good machinability, wear, corrosion, and oxidation resistance (Hu et al., 2024; W. Ye et al., 2024). Various elemental contents and calculations are made to obtain different phases and properties (X. Ye et al., 2024; Zareipour et al., 2024). In addition, multi-phase HEAs exhibit high hardness, excellent wear resistance, oxidation resistance, and corrosion resistance at high temperatures. The addition of Nb to CoCrFeNi HEAs, Wu et al. (T. Wu et al., 2023) and Liu et al. (Liu et al., 2015) demonstrated the transformation from a single face-centered cubic (FCC) phase to a dual-phase configuration containing FCC and Laves phases. The Laves phase, which is formed as a result of Nb enrichment at the grain boundaries, makes a significant contribution to the strengthening of alloys by acting as an effective reinforcing phase at high temperatures. On the other hand, the addition of Nb in high-entropy alloys (HEAs) has a significant impact on the formation of Laves phases. Research has shown that Nb can promote the formation of Laves phases in various HEAs, such as CoCrFeNi and CoCrFeMnNi alloys (Chen et al., 2022). The presence of Nb-rich Laves phases in these alloys contributes to strengthening mechanisms, enhancing the overall mechanical properties of the materials. Moreover, the volume fraction of Laves phases increases with the Nb content, leading to improved ultimate strength but reduced fracture strain in the alloys (Qin et al., 2019). The coherent relationship between Nb-rich Laves phases and the matrix in HEAs demonstrates the potential of Nb to enhance the structural stability and mechanical performance of these advanced materials (Evangeline et al., 2020). Additionally, the segregation of Nb during solidification can promote the formation of Nb-rich Laves phases in Ni-based alloys, affecting their microstructure and corrosion resistance.

The addition of Cu in high-entropy alloys (HEAs) plays a significant role in the formation of Cu-rich phases, impacting the microstructure and mechanical properties. Low Cu concentrations contribute to solid solution strengthening, enhancing both yield strength and ultimate tensile strength (Du et al., 2022). At higher Cu concentrations, nano Cu-rich particles precipitate from the matrix, further increasing the strength properties, but excessive Cu content can lead to the formation of weak continuous Cu-rich phases that reduce the ultimate tensile strength and elongation (X. Zhang et al., 2023). Additionally, the introduction of Cu-rich particles at grain boundaries in nanostructured HEAs

can provide thermal stability and mechanical strength, with the Cu particles acting as grain boundary pinning agents and contributing to high yield strengths and total elongation (Agrawal et al., 2022). Furthermore, strategies to eliminate Cu segregation in HEAs through processing techniques like ball milling and spark plasma sintering have been successful in achieving uniform distribution of Cu, improving both mechanical properties and corrosion resistance while maintaining antibacterial properties. Lastly, in transformation-induced plasticity HEAs, Cu addition can lead to improved ductility, delayed TRIP effect, and enhanced strength through stabilized FCC phases, increased interfaces, and finer grain sizes.

The objective of this study is to investigate the effect of Cu on the microstructural, tribological, and corrosion properties of a high entropy alloy with a composition that causes second-phase formation, such as Nb. The effect of the high positive mixing enthalpy of copper on these properties of the multiphase high entropy alloy CoCuFeNiNb was revealed. The structural, microstructural, tribological, and corrosion properties of the CoCuFeNiNb produced by a vacuum arc melting system were investigated with different approaches.

Materials and Methods

In this study, commercially available Co, Cu, Fe, Ni, and Nb metals with a minimum purity of 99.9% were used to create a multi-phase high entropy alloy. The CoCuFeNiNb equiatomic alloy was prepared by vacuum arc melting these high-purity metals in an argon atmosphere with 99.999% purity. The alloy underwent six remelting cycles, being inverted each time to ensure thorough chemical homogenization. The melting process was conducted in a water-cooled Cu melting pot using a W electrode. After the produced alloy, an optical emission spectrometer (OES) was used to analyze the chemical composition of the HEA. According to the results of the OES analysis, the composition of the prepared high entropy alloy consisted of 16.9 wt.% Fe, 17.8 wt.% Co, 17.7 wt.% Ni, 19.2 wt.% Cu and 28.4 wt.% Nb.

For structural analysis, the sample was sectioned into small pieces. X-ray diffraction (XRD) analysis was performed using a PANalytical Xpert Powder[3] instrument, operating at a step size of 0.013°/s with CuKα radiation in the 2θ range from 10° to 90°. Following standard metallographic procedures, a Zeiss EVO LS10 Scanning Electron Microscope (SEM) was employed to examine the microstructure and visualize corroded and worn surfaces. Elemental ratios in the phases were identified through selective area energy dispersive X-ray spectroscopy (EDX) analysis.

Wear properties were assessed using a pin-on-disc device, with the alloy in contact with 4140 stainless steel under dry sliding conditions. Wear tests were conducted at a sliding speed of 0.3 m/s, over a distance of 4000 m, at room temperature, and under varying loads of 0.25 MPa, 0.5 MPa, and 1.0 MPa. Friction coefficients were measured for each of the three samples. Corrosion properties were examined using Tafel measurements performed with a Gamry Interface 1010E model device. For these measurements, a ternary electrode setup was used, comprising the CoCuFeNiNb high entropy alloy as the working electrode, a graphite rod as the counter electrode, and a saturated calomel electrode as the reference electrode. All corrosion tests were conducted at room temperature in a 3.5 wt% NaCl solution for 3600 s to achieve a stable open circuit potential. Tafel measurements were conducted over a voltage range of -0.5 to 1.5 V with a constant scan rate of 10 mV/s.

Result and Discussion

The X-ray diffraction (XRD) pattern illustrating the structural characteristics of the CoCuFeNiNb alloy is given in Figure 1. Within the XRD pattern of this alloy, one observes the coexistence of face-centered cubic (FCC), body-centered cubic (BCC), and Laves phases. The identification of both FCC and BCC phases in the XRD pattern of the CoCuFeNiNb alloy indicates the presence of a multiphase structure, a feature that could potentially have a beneficial impact on the mechanical and thermal properties of the material. Specifically, the FCC phase is recognized for imparting ductility to the

alloy, whereas the BCC phase is believed to contribute to its hardness and strength. Furthermore, the inclusion of Laves phases in the alloy's XRD pattern might enhance its thermal stability, particularly attributable to the presence of the Nb element, rendering it suitable for applications involving elevated temperatures. In the literature, $CoCrFeNiNiNb_x$ (x: atomic ratio, x = 0, 0.1, 0.2, and 0.3) HEAs (H. Wu et al., 2023), $FeCoCrNiNb_x$ HEAs (Liu et al., 2023), $CoCrFeNiMo_xNby$ HEAs (T. Wu et al., 2023). Some Nb-containing alloys also appear to have Laves phases. The addition of niobium (Nb) to high-entropy alloys (HEAs) has been shown to have significant effects on the microstructure and mechanical properties of HEAs. Studies have demonstrated that increasing Nb content in HEAs leads to the formation of fine eutectic structures, changes the grain shape from columnar to equiaxed, and promotes the stability of body-centered cubic (BCC) phases (Zhang et al., 2022). Furthermore, the presence of Nb can enhance the transformation-induced plasticity (TRIP) effect in BCC HEAs, leading to improved mechanical properties such as work-hardening behavior and increased ductility (Malatji et al., 2020). Additionally, the introduction of Nb in HEAs can induce the formation of hexagonal Laves phases and precipitates, impacting the phase stability and mechanical strength of the alloys (Sunkari et al., 2020). Overall, Nb plays a crucial role in refining microstructures, enhancing mechanical properties, and influencing the phase evolution in HEAs.
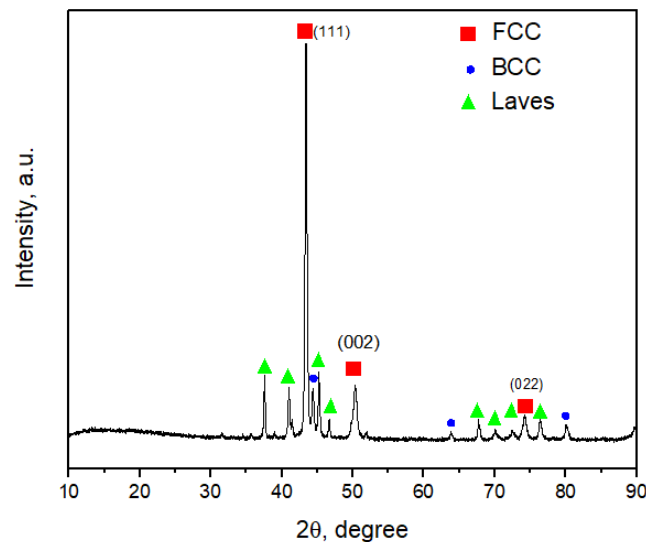
Figure 1. X-ray Diffraction Pattern of CoCuFeNiNb High Entropy Alloy

When examining the microstructure and elemental map analyses of the CoCuFeNiNb high-entropy alloy, understanding why copper (Cu) and niobium (Nb) form second phases requires a comprehension of the microstructural characteristics and thermodynamic factors. Figures 2 and 3 illustrate the microstructure and elemental distribution of this alloy. The data obtained from these figures reveal that phase separations and elemental enrichments are concentrated in specific regions. Figure 2 shows the microstructure of the CoCuFeNiNb high-entropy alloy. Microstructural analysis reveals the presence of different phases. Dark gray areas represent the FCC (Face-Centered Cubic) structure, gray areas represent the BCC (Body-Centered Cubic) structure and light gray areas represent Nb-rich Laves phases. These distinct phases highlight the heterogeneity in the alloy's microstructure. Some parts of the gray areas are Cu-rich regions, indicating that these elements have separated within the alloy. Figure 3 presents the elemental map analysis of the microstructure. The distribution maps of Fe, Cu, Co, Ni, and Nb demonstrate the complexity and non-homogeneous distribution in the alloy's microstructure. The positive mixing enthalpies between copper (Cu) and other elements lead to Cu separating from the matrix phase and forming second phases. Positive mixing enthalpy causes an increase in free energy when two elements mix, leading to thermodynamic instability and phase separations. Cu tends to separate when mixed with elements like Fe, Co, and Ni, making it difficult for Cu to remain dissolved within the matrix. The formation of a Cu-rich phase in high-entropy alloys (HEAs) is influenced by the Cu concentration within the alloy.

Low Cu concentrations (<5 at. %) contribute to solid solution strengthening, enhancing both yield strength and ultimate tensile strength (Du et al., 2022). As the Cu concentration increases to around 7 at. %, nano Cu-rich particles precipitate from the face-centered cubic (FCC) matrix, further strengthening the alloy (Wang et al., 2022). However, when the Cu concentration reaches approximately 13 at.%, a weak continuous Cu-rich phase forms between dendrites, which can lead to early fracture and a significant decrease in ultimate tensile strength and elongation (Kai-Le et al., 2023). On the other hand, Cu and Nb have different atomic sizes compared to other elements. These size differences create stress fields in the microstructure, leading to phase separations. Atomic size differences can cause Cu and Nb to cluster around larger or smaller atoms, forming distinct phases (Freudenberger et al., 2004; Park et al., 2016). In the CoCuFeNiNb high-entropy alloy, the formation of second phases by copper (Cu) and niobium (Nb) occurs due to positive mixing enthalpies, atomic size differences, crystal structure mismatches, thermodynamic instability, and chemical properties. These factors explain the heterogeneity and phase separations in the alloy's microstructure. The microstructural and elemental analyses in Figures 2 and 3 support these theoretical explanations and visually reveal the reasons for Cu and Nb forming separate phases. These phase separations significantly impact the mechanical and physical properties of the alloy, and should be considered in engineering applications.
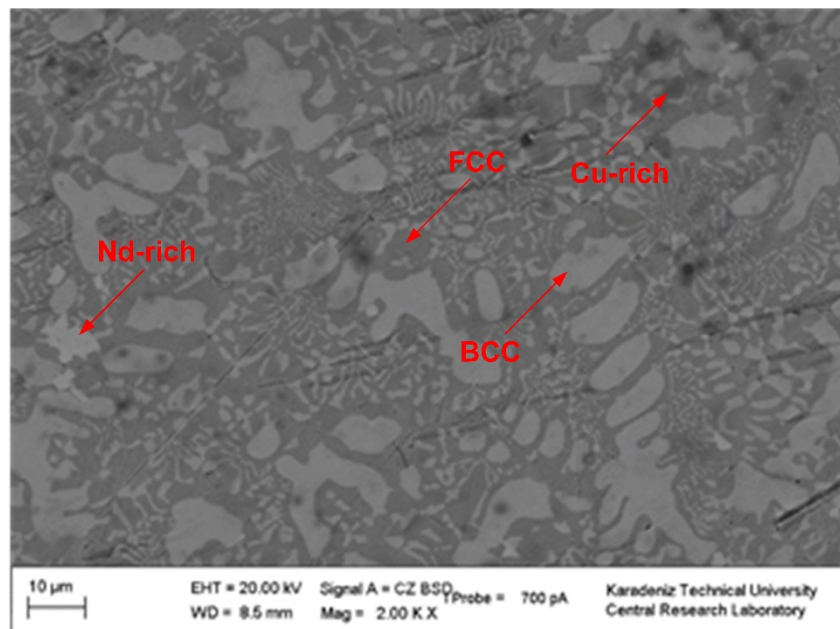
Figure 2. SEM Image of CoCuFeNiNb High Entropy Alloy

Elementler	Wt %
Nb	24.0
Fe	23.0
Cu	20.9
Ni	16.4
Co	15.7
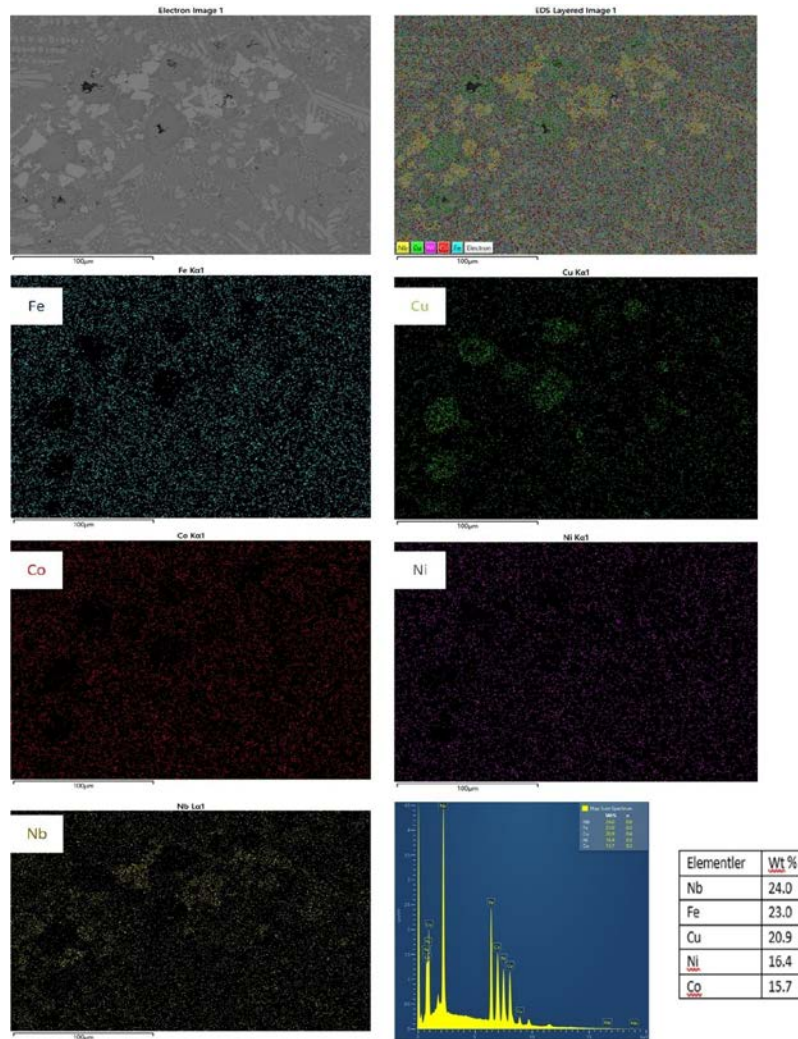
Figure 3. EDS Map Analysis Results of CoCuFeNiNb High Entropy Alloy

The graph in Figure 4 illustrates the friction coefficient as a function of time under different loads for the CoCuFeNbNi high-entropy alloy in a dry sliding condition. Across all loads, the friction coefficient demonstrates a very stable curve. However, a minor fluctuation is observed under the 1 MPa load up to approximately 500 seconds, after which it stabilizes. This fluctuation can be attributed to various factors including phase composition, inhomogeneities in the alloy's microstructure, the formation of cracks on the worn surface, oxidation, or the development of delamination layers. The high-entropy alloy CoCuFeNbNi is composed of multiple elements that can form various phases, including FCC, BCC, and Laves phases. The presence of Cu and the formation of Nb-rich Laves phases can lead to microstructural inhomogeneities. These phases have different mechanical properties and responses to wear, which can contribute to fluctuations in the friction coefficient. For instance, Cu tends to segregate due to its positive mixing enthalpy with other elements, leading to regions within the alloy that are richer in Cu and potentially softer. This segregation can cause variations in the local hardness and wear resistance of the alloy, affecting the friction behavior over time. Research indicates that the presence of copper can lead to segregation in HEAs, affecting mechanical properties and corrosion resistance (Mukanov et al., 2023). Strategies such as ball milling and spark plasma sintering have been proposed to eliminate Cu segregation in HEAs, resulting in improved strength, plasticity, and corrosion resistance. Additionally, the distribution of Cu elements in HEAs becomes more uniform with the dissolution of the Cu-rich phase, leading to enhanced mechanical properties and corrosion resistance (Cheng et al., 2022).

During the initial period under the 1 MPa load, microstructural inhomogeneities might lead to the formation of cracks on the worn surface. These cracks can act as initiation points for delamination, where layers of the material start to peel off due to repeated sliding contact. This process can cause temporary increases in the friction coefficient as new, rough surfaces are exposed. Over time, these cracks may propagate and merge, leading to a more uniform worn surface that stabilizes the friction coefficient. Another factor contributing to the fluctuation in the friction coefficient is oxidation. During sliding, the high contact pressures and temperatures can promote the formation of oxide layers on the alloy surface. These oxides can be beneficial by forming a protective layer that reduces direct metal-to-metal contact, but they can also break away and contribute to wear debris. The formation and removal of these oxide layers can cause variations in the friction coefficient until a steady-state condition is achieved where the rate of oxide formation and removal reaches equilibrium. As the load increases, the interaction between the sliding surfaces intensifies. Higher loads lead to greater contact pressures, which can increase the extent of plastic deformation and material transfer between the surfaces. This increased interaction can result in more pronounced wear debris, oxide layer formation, and localized cracking, all contributing to the observed fluctuations in friction. Under higher loads, such as 1 MPa, these effects are more significant due to the greater forces involved. The overall trend observed is that the friction coefficient increases with increasing load. At the end of the 4000-second test duration, the average friction coefficients for 0.25 MPa, 0.5 MPa, and 1.0 MPa loads are approximately 0.28, 0.5, and 0.78, respectively. This increase in friction coefficient with load can be explained by several factors: With increasing load, the contact pressure between the sliding surfaces increases. This higher pressure enhances the real area of contact, leading to more significant adhesion and increased friction. Higher loads result in greater plastic deformation of the alloy's surface. This deformation can increase the surface roughness and the mechanical interlocking between the sliding surfaces, contributing to a higher friction coefficient. At higher loads, the amount of wear debris generated increases. These debris particles can become entrapped between the sliding surfaces, acting as abrasive particles that further increase the friction coefficient. The formation and removal of oxide layers are more pronounced under higher loads. These oxides can initially act as a solid lubricant, reducing friction, but their breakdown and removal can expose fresh metal surfaces that increase friction until a new oxide layer forms. The stability of the friction coefficient under different loads indicates the alloy's robustness in dry sliding conditions. However, the initial fluctuation observed at 1 MPa suggests that microstructural factors and surface interactions play significant roles in the alloy's tribological performance. The increase in friction coefficient with load highlights the need to consider these effects in applications where the alloy will be subjected to varying loads and sliding conditions. Overall, the CoCuFeNbNi high-entropy alloy exhibits stable frictional behavior under different loads, with specific factors contributing to initial fluctuations at higher loads. Understanding these factors is crucial for optimizing the alloy's performance in practical applications, ensuring reliable and efficient operation under various tribological conditions.
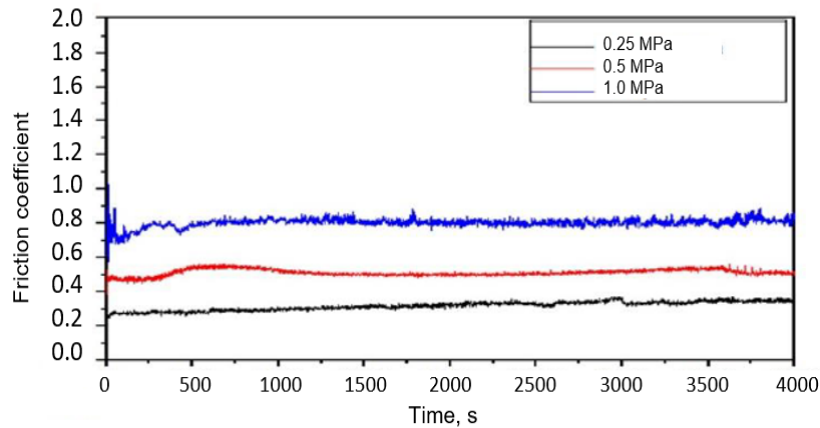
Figure 4. Coefficient of Friction-Time Plot of CoCuFeNiNb High Entropy Alloy under 0.25 MPa, 0.5 MPa, and 1 MPa Load

The wear surfaces of the CoCuFeNiNb high-entropy alloy, which is shown in Figure 5, were analyzed under various contact pressures (0.25 MPa, 0.5 MPa, and 1 MPa) to understand the relationship between wear behavior and contact pressure. The results reveal a direct correlation between contact pressure and the wear characteristics of the alloy. Under a low contact pressure of 0.25 MPa, the wear surface predominantly exhibited abrasion marks and small pits. These observations suggest that the wear mechanism at this pressure is primarily abrasive wear. The friction coefficient was measured to be approximately 0.28, indicating good tribological performance under low-pressure conditions. The presence of abrasion marks suggests that the material removal process was relatively uniform, with minimal severe damage or plastic deformation occurring on the surface. The small pits observed could be attributed to minor adhesive wear or localized micro-plowing effects. At an intermediate contact pressure of 0.5 MPa, the wear surface showed a combination of abrasion and delamination marks. The formation of delamination layers was also noticeable. The friction coefficient at this pressure increased slightly to around 0.5. This increase indicates a transition in the wear mechanism due to the higher contact pressure. The presence of both abrasion and delamination marks suggests that the alloy surface experienced higher stress levels, leading to the initiation and propagation of subsurface cracks. These cracks eventually caused the material to delaminate, creating a rougher surface texture and increasing the friction coefficient. The delamination layers are indicative of repeated mechanical loading and fatigue, which are characteristic of intermediate wear conditions. Under a high contact pressure of 1 MPa, the wear surface exhibited pronounced delamination marks, regions of plastic deformation, and intense abrasion marks. The friction coefficient significantly increased to approximately 0.78. This substantial increase in the friction coefficient indicates a more severe wear regime. The pronounced delamination marks suggest extensive subsurface cracking and material spalling. The regions of plastic deformation indicate that the material underwent significant mechanical strain, leading to the permanent deformation of the surface. The intense abrasion marks at this pressure are likely due to the high contact stress, which facilitates the removal of material in the form of wear debris. The combination of these wear mechanisms under high-pressure results in a rough and damaged surface, contributing to the higher friction coefficient. The observed wear behavior and friction coefficients under different contact pressures provide valuable insights into the performance of the CoCuFeNiNb high-entropy alloy in various tribological conditions. The alloy shows good wear resistance and low friction under low contact pressure (0.25 MPa). The primary wear mechanism is abrasion, with minimal severe damage, suggesting that the alloy can perform well in applications where contact stresses are relatively low. At medium contact pressure (0.5 MPa), the wear behavior changes, with both abrasion and delamination contributing to material removal. The increase in friction coefficient indicates that while the alloy can still perform adequately, there is a higher degree of wear and surface damage. Applications involving intermediate contact pressures should consider this transition in wear mechanisms. Under high contact pressure (1 MPa), the alloy experiences severe wear, with

significant delamination, plastic deformation, and intense abrasion. The high friction coefficient reflects the extensive surface damage and material loss. This suggests that the alloy may require additional considerations, such as surface treatments or lubrication, to improve its performance in high-stress applications.
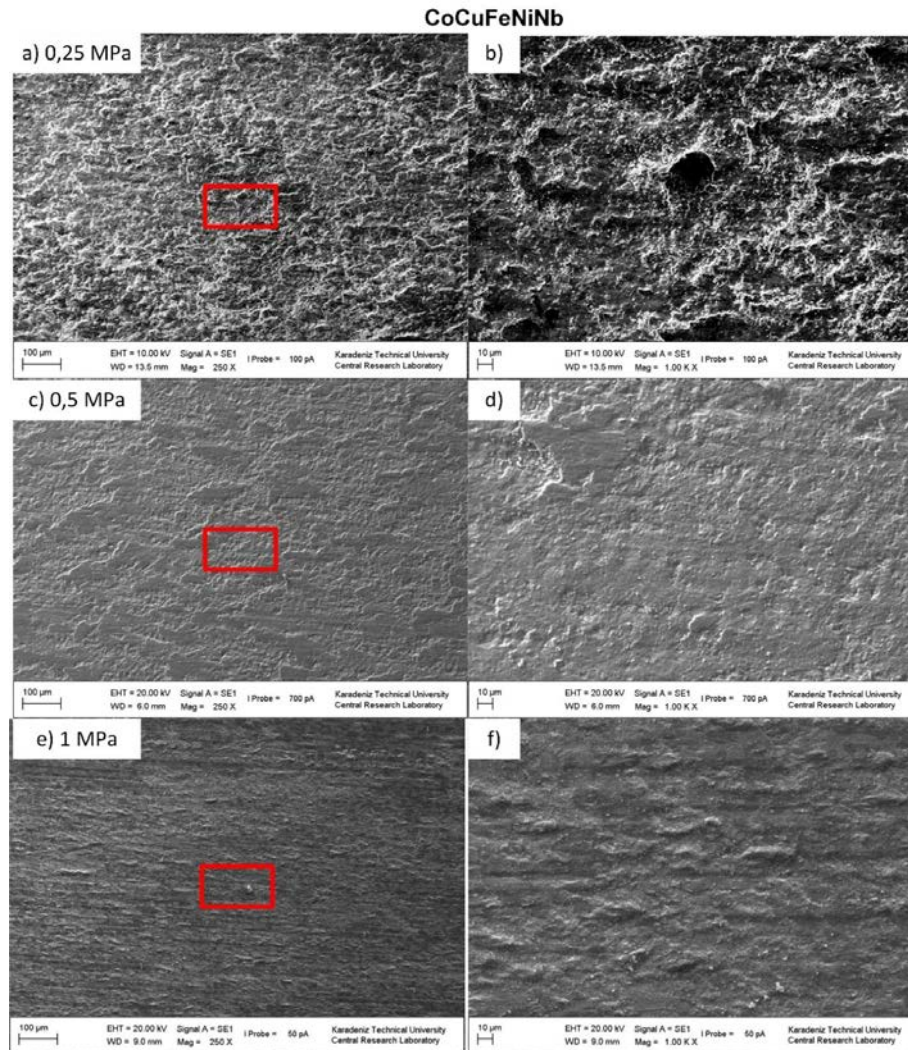
Figure 5. SEM Morphologies of the Worn surfaces of CoCuFeNiNb High Entropy Alloy under Loads of (a) and (b) 0.25 MPa, (c) and (d) 0.5 MPa, (e) and (f) 1.0 MPa

Figure 6 shows the wear particles of the CoCuFeNiNb high-entropy alloy under a pressure of 1 MPa. Given that the wear particles are similar across different loads, only the wear particles under the 1 MPa load are presented. The morphology and size of the wear particles in the image are noteworthy. Most particles have irregular shapes and varying sizes, indicating that the wear mechanism is associated with multiple processes such as abrasion and delamination. Specifically, the heterogeneous distribution and size differences of the particles suggest that material loss on the wear surface originates from microstructural weaknesses and stress concentrations that form under load. Additionally, some particles exhibit agglomeration, indicating the presence of plastic deformation and large material masses detached from the surface. The obtained images reveal that the wear particles exhibit irregular shapes and different sizes. This variety reflects the heterogeneous nature of the wear process and the involvement of various mechanisms. The majority of the particles having irregular shapes indicate the influence of abrasive wear and delamination. Abrasive wear involves the continuous removal of material from the surface due to mechanical interactions, causing microscopic-level wear. The heterogeneous distribution and size differences of the particles show that different wear mechanisms are effective simultaneously on the material surface: Hard particles

on the material surface create scratches, leading to material loss. This process results in the formation of irregular and varying-sized particles. Under high pressure, cracks form in the subsurface layers of the material and propagate to the surface, causing the detachment of material layers. This process is particularly effective in the formation of large and irregular particles.
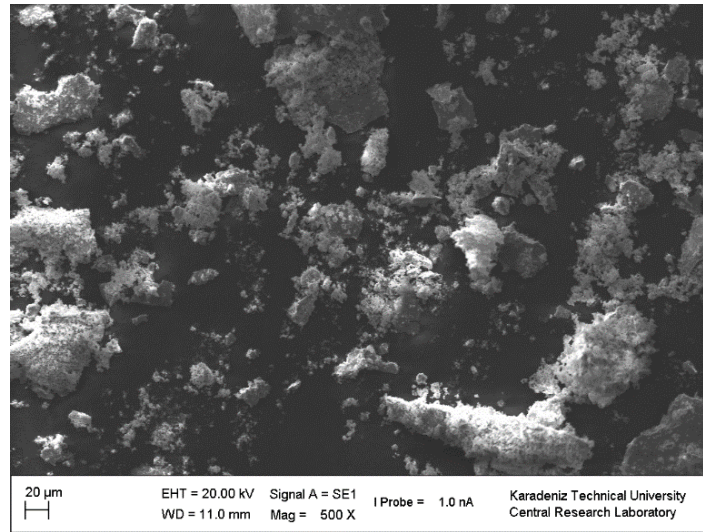
Figure 6. Wear Particles of CoCuFeNiNb High Entropy Alloy under 1 MPa

Figure 7 presents the potentiodynamic polarization curve of the CoCuFeNiNb high-entropy alloy in a 3.5% NaCl solution. From this curve, the corrosion potential (Ecorr) is determined to be -0.236 V, and the corrosion current density (icorr) is found to be 1.89×10^{-5} A/cm². These values provide insights into the corrosion behavior of the CoCuFeNiNb high-entropy alloy. The corrosion potential, Ecorr, is an important parameter that indicates the susceptibility of the alloy to corrosion. An Ecorr value of -0.236 V suggests that the alloy has a moderate tendency to undergo corrosion in the NaCl solution. This potential reflects the protective characteristics of the passive film on the alloy's surface and its resistance to anodic and cathodic reactions. A more positive Ecorr generally indicates a lower tendency for the material to corrode, while a more negative value indicates a higher tendency. The corrosion current density, icorr, represents the rate of corrosion of the alloy. The value of 1.89×10^{-5} A/cm² indicates that the alloy has a low corrosion rate, implying slow corrosion progression. A low icorr value is desirable as it means that the material is more resistant to corrosion and can maintain its integrity over a longer period when exposed to corrosive environments. The obtained Ecorr and icorr values suggest that the CoCuFeNiNb high-entropy alloy can be safely used in NaCl solutions and similar corrosive environments. The low corrosion rate indicates that the alloy can withstand corrosive attacks without significant degradation. This makes it suitable for applications where exposure to saline environments is common, such as in marine engineering or chemical processing. The general shape of the polarization curve further indicates the formation of a stable passive film on the alloy's surface. This passive film acts as an effective barrier against corrosion processes. The formation of such a film is crucial as it prevents the underlying metal from coming into direct contact with the corrosive environment, thereby significantly reducing the corrosion rate. The stability of this passive film is evident from the polarization behavior, where a stable and protective layer forms, maintaining the integrity of the alloy.
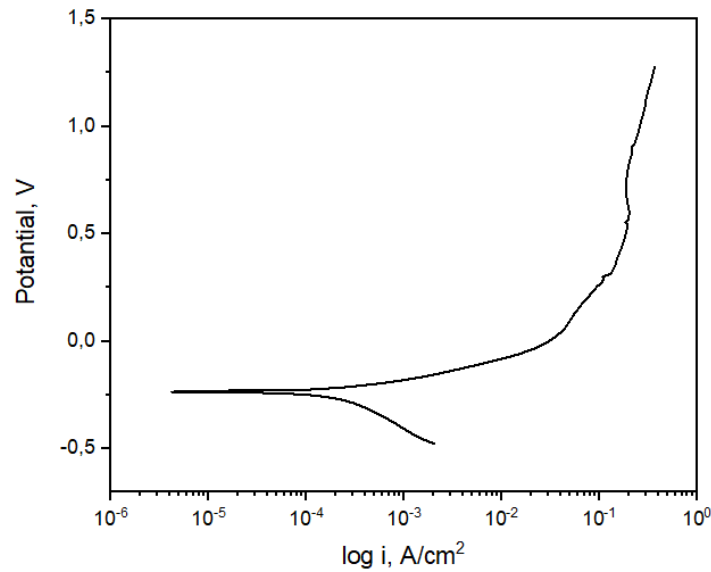
Figure 7. Potentiodynamic Polarisation Curve of CoCuFeNiNb High Entropy Alloy

The SEM image obtained after the electrochemical corrosion tests of the CoCuFeNiNb high-entropy alloy, shown in Figure 8 at 1000x magnification with a 10 μm scale bar, reveals the morphological changes on the surface. The image depicts microstructural changes and damage that occurred on the alloy's surface post-corrosion. Notable features include widespread roughness, cracks, surface irregularities, and pits. These morphological changes indicate material loss from the surface during the corrosion process. The observed pits and the formation of corrosion products are associated with the material detaching from the surface and then re-depositing. Additionally, these pits represent localized areas where corrosion has intensified, typically due to the formation of local galvanic cells induced by Cl^- ions on the surface. Such localized corrosion can result from microstructural heterogeneities and electrochemical potential differences between various phases within the material.
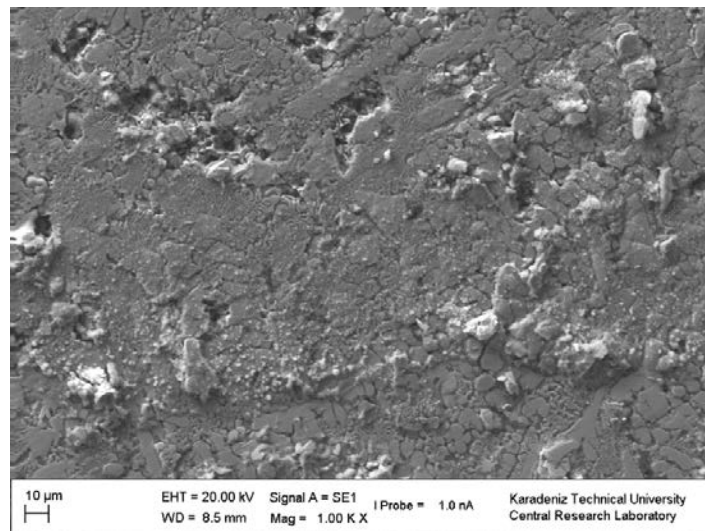
Figure 8. Surface Morphology Image Obtained after Electrochemical Measurement

Conclusion

This study provides a comprehensive evaluation of the structural, tribological, and corrosion properties of the CoCuFeNiNb high-entropy alloy. XRD and SEM analyses revealed that the alloy contains FCC, BCC, and Laves phases, which positively influence its tribological properties. Wear tests show that the alloy performs well under low and medium pressures but requires careful

consideration under high pressures. Corrosion tests indicate that the alloy exhibits good corrosion resistance in NaCl solution and forms a stable passive film on its surface. Some important results obtained in the study are summarized below.

- The CoCuFeNiNb alloy exhibits a multiphase structure consisting of FCC, BCC, and Laves phases.

- The formation of second phases by copper (Cu) and niobium (Nb) in the CoCuFeNiNb high-entropy alloy, specifically the FCC, BCC, and Nb-rich Laves phases, is driven by positive mixing enthalpies, atomic size differences, crystal structure mismatches, thermodynamic instability, and chemical properties, resulting in significant microstructural heterogeneity and phase separations.

- The wear tests show that the alloy has an average friction coefficient of 0.28 under a 0.25 MPa load, 0.5 under a 0.5 MPa load, and 0.78 under a 1 MPa load, indicating good performance under low and medium pressures but requiring careful consideration under high pressures.

- Corrosion tests reveal that the alloy has a corrosion potential (Ecorr) of -0.236 V and a corrosion current density (icorr) of 1.89×10^{-5} A/cm² in a 3.5% NaCl solution, indicating good corrosion resistance and the formation of a stable passive film, making it suitable for use in corrosive environments.

Author Contribution

Sefa Emre Sünbül, prepared the experimental procedures and followed the experimental process, prepared the manuscript, and analyzed the data. *Kürşat İçin*, prepared the experimental procedures and followed the experimental process, prepared the manuscript, and analyzed the data.

Ethics Statement

There are no ethical problems regarding the publication of this paper.

Conflict of Interest

The authors state that there is no conflict of interest.

ORCID

Sefa Emre Sünbül https://orcid.org/0000-0002-2648-9268

Kürşat İçin https://orcid.org/0000-0002-5160-6753

References

Agrawal, P., Gupta, S., Shukla, S., Nene, S. S., Thapliyal, S., Toll, M. P., & Mishra, R. S. (2022). Role of Cu addition in enhancing strength-ductility synergy in transforming high entropy alloy. *Materials & Design, 215*, 110487. https://doi.org/10.1016/j.matdes.2022.110487

Cao, B. X., Wang, C., Yang, T., & Liu, C. T. (2020). Cocktail effects in understanding the stability and properties of face-centered-cubic high-entropy alloys at ambient and cryogenic temperatures. *Scripta Materialia, 187*, 250-255. https://doi.org/10.1016/j.scriptamat.2020.06.008

Chen, T. K., Shun, T. T., Yeh, J. W., & Wong, M. S. (2004). Nanostructured nitride films of multi-element high-entropy alloys by reactive DC sputtering [Article]. *Surface and Coatings Technology*, *188-189*(1-3 SPEC.ISS.), 193-200. https://doi.org/10.1016/j.surfcoat.2004.08.023

Chen, X.-g., Qin, G., Gao, X.-f., Chen, R.-r., Song, Q., & Cui, H.-z. (2022). Strengthening CoCrFeNi high-entropy alloy by Laves and boride phases. *China Foundry, 19*(6), 457-463. https://doi.org/10.1007/s41230-022-1007-4

Cheng, Z., Wang, S., Wu, G., Gao, J., Yang, X., & Wu, H. (2022). Tribological properties of high-entropy alloys: A review. I*nternational Journal of Minerals, Metallurgy and Materials, 29*(3), 389-403. https://doi.org/10.1007/s12613-021-2373-4

Dada, M., Popoola, P., & Mathe, N. (2023). Recent advances of high entropy alloys for aerospace applications: A review. *World Journal of Engineering, 20*(1), 43-74. https://doi.org/10.1108/WJE-01-2021-0040

Dewangan, S. K., Mangish, A., Kumar, S., Sharma, A., Ahn, B., & Kumar, V. (2022). A review on High-Temperature Applicability: A milestone for high entropy alloys. *Engineering Science and Technology, an International Journal, 35*, 101211. https://doi.org/10.1016/j.jestch.2022.101211

Du, C., Hu, L., Pan, Q., Chen, K., Zhou, P., & Wang, G. (2022). Effect of Cu on the strengthening and embrittling of an FeCoNiCr-xCu HEA. *Materials Science and Engineering: A, 832*, 142413. https://doi.org/10.1016/j.msea.2021.142413

Evangeline, A., Sathiya, P., & Arivazhagan, B. (2020). Laves Phase Formation and Segregation of Nb in Ni–Cr–Mo Superalloy over 316L by Hot Wire (HW) TIG Cladding Process. A*rabian Journal for Science and Engineering, 45*(11), 9685-9698. https://doi.org/10.1007/s13369-020-04873-0

Freudenberger, J., Botcharova, E., & Schultz, L. (2004). Formation of the microstructure in Cu-Nb alloys. J*ournal of Materials Science, 39*(16), 5343-5345. https://doi.org/10.1023/B:JMSC.0000039241.01005.c6

Hu, J., Yang, K., Wang, Q., Zhao, Q. C., Jiang, Y. H., & Liu, Y. J. (2024). Ultra-long life fatigue behavior of a high-entropy alloy. *International Journal of Fatigue, 178*, 108013. https://doi.org/10.1016/j.ijfatigue.2023.108013

Kai-Le, W., Wen-Kui, Y., Xin-Cheng, S., Hua, H., & Yu-Hong, Z. (2023). Phase field method to study the mechanism of Cu-rich phase precipitation in AlxCuMnNiFe high-entropy alloy. A*cta Physica Sinica, 72*. https://doi.org/10.7498/aps.72.20222439

Liu, C., Gao, Y., Chong, K., Guo, F., Wu, D., & Zou, Y. (2023). Effect of Nb content on the microstructure and corrosion resistance of FeCoCrNiNbx high-entropy alloys in chloride ion environment. *Journal of Alloys and Compounds, 935*, 168013. https://doi.org/10.1016/j.jallcom.2022.168013

Liu, W. H., He, J. Y., Huang, H. L., Wang, H., Lu, Z. P., & Liu, C. T. (2015). Effects of Nb additions on the microstructure and mechanical property of CoCrFeNi high-entropy alloys. *Intermetallics, 60*, 1-8. https://doi.org/10.1016/j.intermet.2015.01.004

Malatji, N., Popoola, A. P. I., Lengopeng, T., & Pityana, S. (2020). Effect of Nb addition on the microstructural, mechanical and electrochemical characteristics of AlCrFeNiCu high-entropy alloy. I*nternational Journal of Minerals, Metallurgy and Materials, 27*(10), 1332-1340. https://doi.org/10.1007/s12613-020-2178-x

Man, J., Wu, B., Duan, G., Zhang, L., Wan, G., Zhang, L., Zou, N., & Liu, Y. (2022). The synergistic addition of Al, Ti, Mo and W to strengthen the equimolar CoCrFeNi high-entropy alloy via thermal-mechanical processing. *Journal of Alloys and Compounds, 902*, 163774. https://doi.org/10.1016/j.jallcom.2022.163774

Miracle, D. B., & Senkov, O. N. (2017). A critical review of high entropy alloys and related concepts. *Acta Materialia, 122*, 448-511. https://doi.org/10.1016/j.actamat.2016.08.081

Mukanov, S., Loginov, P., Fedotov, A., Bychkova, M., Antonyuk, M., & Levashov, E. (2023). The effect of copper on the microstructure, wear and corrosion resistance of cocrcufeni high-entropy alloys manufactured by powder metallurgy. *Materials, 16*(3), 1178. https://doi.org/10.3390/ma16031178

Park, H. J., Na, Y. S., Hong, S. H., Kim, J. T., Kim, Y. S., Lim, K. R., Park, J. M., & Kim, K. B. (2016). Phase evolution, microstructure and mechanical properties of equi-atomic substituted TiZrHfNiCu and TiZrHfNiCuM (M = Co, Nb) high-entropy alloys. *Metals and Materials International, 22*(4), 551-556. https://doi.org/10.1007/s12540-016-6034-5

Qin, G., Li, Z., Chen, R., Zheng, H., Fan, C., Wang, L., Su, Y., Ding, H., Guo, J., & Fu, H. (2019). CoCrFeMnNi high-entropy alloys reinforced with Laves phase by adding Nb and Ti elements. J*ournal of Materials Research, 34*(6), 1011-1020. https://doi.org/10.1557/jmr.2018.468

Rashidy Ahmady, A., Ekhlasi, A., Nouri, A., Haghbin Nazarpak, M., Gong, P., & Solouk, A. (2023). High entropy alloy coatings for biomedical applications: A review. *Smart Materials in Manufacturing, 1*, 100009. https://doi.org/10.1016/j.smmf.2022.100009

Sonar, T., Ivanov, M., Trofimov, E., Tingaev, A., & Suleymanova, I. (2024). An overview of microstructure, mechanical properties and processing of high entropy alloys and its future perspectives in aeroengine applications. *Materials Science for Energy Technologies, 7*, 35-60. https://doi.org/10.1016/j.mset.2023.07.004

Sunkari, U., Reddy, S. R., Athira, K. S., Chatterjee, S., & Bhattacharjee, P. P. (2020). Effect of niobium alloying on the microstructure, phase stability and mechanical properties of CoCrFeNi2.1Nbx high entropy alloys: Experimentation and thermodynamic modeling. *Materials Science and Engineering: A, 793*, 139897. https://doi.org/10.1016/j.msea.2020.139897

Verma, V., Belcher, C. H., Apelian, D., & Lavernia, E. J. (2024). Diffusion in high entropy alloy systems – A review. *Progress in Materials Science, 142*, 101245. https://doi.org/10.1016/j.pmatsci.2024.101245

Wang, H., He, Q., Gao, X., Shang, Y., Zhu, W., Zhao, W., Chen, Z., Gong, H., & Yang, Y. (2024). Multifunctional High Entropy Alloys Enabled by Severe Lattice Distortion. *Advanced Materials, 36*(17), 2305453. https://doi.org/10.1002/adma.202305453

Wang, L., Zhang, L., Lu, X., Wu, F., Sun, X., Zhao, H., & Li, Q. (2023). Surprising cocktail effect in high entropy alloys on catalyzing magnesium hydride for solid-state hydrogen storage. C*hemical Engineering Journal, 465*, 142766. https://doi.org/10.1016/j.cej.2023.142766

Wang, Z., Lan, N., Zhang, Y., & Deng, W. (2022). Microstructure and properties of MAO-Cu/Cu-(HEA)N composite coatings on titanium alloy. *Coatings, 12*(12), 1877. https://doi.org/10.3390/coatings12121877

Wu, H., Zhang, S., Wu, C. L., Zhang, C. H., Sun, X. Y., & Bai, X. L. (2023). Electrochemical corrosion behavior in sulfuric acid solution and dry sliding friction and wear properties of laser-cladded CoCrFeNiNbx high entropy alloy coatings. *Surface and Coatings Technology, 460*, 129425. https://doi.org/10.1016/j.surfcoat.2023.129425

Wu, T., Yu, L., Chen, G., Wang, R., Xue, Y., Lu, Y., & Luan, B. (2023). Effects of Mo and Nb on the microstructure and high temperature oxidation behaviors of CoCrFeNi-based high entropy alloys. *Journal of Materials Research and Technology, 27*, 1537-1549. https://doi.org/10.1016/j.jmrt.2023.10.058

Yang, T., Xia, S., Liu, S., Wang, C., Liu, S., Zhang, Y., Xue, J., Yan, S., & Wang, Y. (2015). Effects of AL addition on microstructure and mechanical properties of AlxCoCrFeNi High-entropy alloy. *Materials Science and Engineering: A, 648*, 15-22. https://doi.org/10.1016/j.msea.2015.09.034

Ye, W., Zhou, Q., Shi, Y., Xie, M., Chen, B., Wang, H., & Liu, W. (2024). Robust wear performance of graphene-reinforced high entropy alloy composites. *Carbon, 224,* 119040. https://doi.org/10.1016/j.carbon.2024.119040

Ye, X., Diao, Z., Lei, H., Wang, L., Li, Z., Li, B., Feng, J., Chen, J., Liu, X., & Fang, D. (2024). Multi-phase FCC-based composite eutectic high entropy alloy with multi-scale microstructure. *Materials Science and Engineering: A, 889*, 145815. https://doi.org/10.1016/j.msea.2023.145815

Yeh, J. W., Chen, S. K., Lin, S. J., Gan, J. Y., Chin, T. S., Shun, T. T., Tsau, C. H., & Chang, S. Y. (2004). Nanostructured High-Entropy Alloys with Multiple Principal Elements: Novel Alloy Design Concepts and Outcomes. A*dvanced Engineering Materials, 6*(5), 299-303. https://doi.org/10.1002/adem.200300567

Yu, B., Ren, Y., Zeng, Y., Ma, W., Morita, K., Zhan, S., Lei, Y., Lv, G., Li, S., & Wu, J. (2024). Recent progress in high-entropy alloys: A focused review of preparation processes and properties. *Journal of Materials Research and Technology, 29*, 2689-2719. https://doi.org/10.1016/j.jmrt.2024.01.246

Zareipour, F., Shahmir, H., & Huang, Y. (2024). Formation and significance of topologically close-packed Laves phases in refractory high-entropy alloys. *Journal of Alloys and Compounds, 986*, 174148. https://doi.org/10.1016/j.jallcom.2024.174148

Zhang, C., Huang, L., Li, S., Li, K., Lu, S., & Li, J. (2023). Improved corrosion resistance of laser melting deposited CoCrFeNi-series high-entropy alloys by Al addition. *Corrosion Science, 225*, 111599. https://doi.org/10.1016/j.corsci.2023.111599

Zhang, F., Xiang, C., Han, E.-H., & Zhang, Z. (2022). Effect of Nb Content on Microstructure and Mechanical Properties of Mo0.25V0.25Ti1.5Zr0.5Nbx High-Entropy Alloys. *Acta Metallurgica Sinica (English Letters), 35*(10), 1641-1652. https://doi.org/10.1007/s40195-022-01399-2

Zhang, X., Yu, Y., Ren, B., Liu, Z., Li, T., Wang, L., & Qiao, Z. (2023). Design of a novel CoCrFeNiCu0.3 high entropy alloy with desirable mechanical, corrosion and anti-bacterial properties via adjusting Cu distribution. *Materials Today Communications, 35*, 105946. https://doi.org/10.1016/j.mtcomm.2023.105946